

Downregulation of *Lnc-Spry1* mediates TGF- β -induced epithelial–mesenchymal transition by transcriptional and posttranscriptional regulatory mechanisms

Cristina Rodríguez-Mateo¹, Belén Torres¹, Gabriel Gutiérrez² and José A Pintor-Toro^{*1}

Long non-coding RNAs (lncRNAs) are a class of regulatory genes that participate in a wide range of biological processes, including proliferation, differentiation and development, as well as in a broad spectrum of diseases. Although the role of lncRNAs in TGF- β -induced epithelial-to-mesenchymal transition (EMT) has been well established, little is known about the role of lncRNAs as immediate-early regulators of EMT. Here *Lnc-Spry1* is identified as an immediate-early regulator of EMT that is downregulated by TGF- β . It is also found that knockdown of *Lnc-Spry1* promotes a mesenchymal-like phenotype and results in increased cell migration and invasion. In addition, it is shown that *Lnc-Spry1* depletion preferentially affects the expression of TGF- β -regulated gene targets. Moreover, *Lnc-Spry1* associates with U2AF65 splicing factor, suggesting a role in alternative splicing. Depletion of *Lnc-Spry1* induces, as TGF- β , isoform switching of fibroblast growth factor receptors, resulting in FGF-2-sensitive cells. Taken together, these results show that *Lnc-Spry1* could act as an early mediator of TGF- β signaling and reveal different roles for a lncRNA in modulating transcriptional and posttranscriptional gene expression.

Cell Death and Differentiation (2017) 24, 785–797; doi:10.1038/cdd.2017.9; published online 10 February 2017

EMT is a basic cellular process in which epithelial cells lose their epithelial characteristics and take on properties of mesenchymal cells. During EMT, epithelial cells lose their cell–cell junctions and the epithelial apical–basal polarity. The actin cytoskeleton is reorganized and cells acquire migratory and invasive properties.^{1–3} This process is essential in the generation of tissues and organs during embryogenesis, during wound healing and is associated with pathologies, such as fibrosis and cancer. In carcinomas, cancer cells can undergo EMT to escape the primary tumor, invade surrounding tissues and colonize remote sites via blood or lymphatic routes generating metastases.^{4–6}

The EMT program can be activated efficiently and rapidly in epithelial cells in response to soluble factors or cytokines, including epidermal growth factor, fibroblast growth factors (FGFs) and transforming growth factors (TGF- β s). TGF- β may induce EMT through distinct signaling mechanisms causing substantial changes in gene expression. These changes involve three families of transcription factors: the zinc finger Snail, Zeb, and basic helix–loop–helix families.⁷

Beyond the well-established transcriptional reprogramming during EMT, posttranscriptional mechanisms, such as regulation by alternative pre-mRNA splicing and regulation by non-coding RNA, have an important role and provide an additional layer of complexity on the gene regulation during EMT.^{8–12}

The mammalian genome encodes many thousands of lncRNAs, a class of transcripts >200 nucleotides with limited protein-coding potential.¹³ They can act as molecular signals, tethers, decoys, guides or scaffolds at every level of gene

regulation in a wide range of biological processes.^{14–16} Although transcription factors, microRNAs and signaling pathways that control EMT have been studied intensively, lncRNAs that may regulate this process in an immediate-early phase have not been identified. Several lncRNAs have been reported to be involved in EMT;^{17–21} however, these lncRNAs have been identified in cells treated with TGF- β for days or in cells stably expressing an EMT-inducer transcription factor. Here we profiled immediate-early changes of lncRNAs in NMuMG cells following TGF- β treatment. This study reports the identification of a lncRNA located adjacent to the mouse *Spry1* gene, which was named *Lnc-Spry1*, early downregulated by TGF- β . Decreased *Lnc-Spry1* levels induce a mesenchymal-like phenotype leading to increased cell migration and invasion. *Lnc-Spry1* was found to interact with U2AF65 RNA splicing regulator, suggesting a posttranscriptional regulation of EMT-associated genes. Taken together, our findings indicate that *Lnc-Spry1* modulates early transcriptional expression and alternative splicing (AS) of genes involved in the EMT process.

Results

TGF- β -mediated EMT regulates the expression of lncRNAs. Transcription factors regulating EMT are induced early. We hypothesized that lncRNAs with a differential expression during early EMT could represent putative EMT regulators. To identify such lncRNAs, transcriptional profiling was performed in untreated NMuMG mammary epithelial

¹Department of Cell Signaling, Centro Andaluz de Biología Molecular y Medicina Regenerativa (CABIMER-CSIC), Avda Américo Vespucio s/n, Seville 41092, Spain and

²Department of Genetics, Seville University, Seville 41080, Spain

*Corresponding author: JA Pintor-Toro, Department of Cell Signaling Centro Andaluz de Biología Molecular y Medicina Regenerativa (CABIMER-CSIC), Avda Américo Vespucio s/n Isla de la Cartuja, Sevilla 41092, Spain. Tel: +34 954 467 995; Fax: +34 954 46 16 64; E-mail: jose.pintor@cabimer.es

Received 16.6.16; revised 16.12.16; accepted 11.1.17; Edited by X Lu; published online 10.2.2017

cells, a widely employed model to study TGF- β -induced EMT, and NMuMG cells treated with TGF- β for 2 h using chips that cover 31 423 annotated lncRNAs and also 25 376 protein-coding transcripts. Fold change values >2 and P -values

<0.05 were set as the filtering criteria to analyze differentially expressed RNAs (Supplementary Figure S1). At this time, microarray results indicated that TGF- β treatment for 2 h led to EMT gene expression signature²² (Supplementary

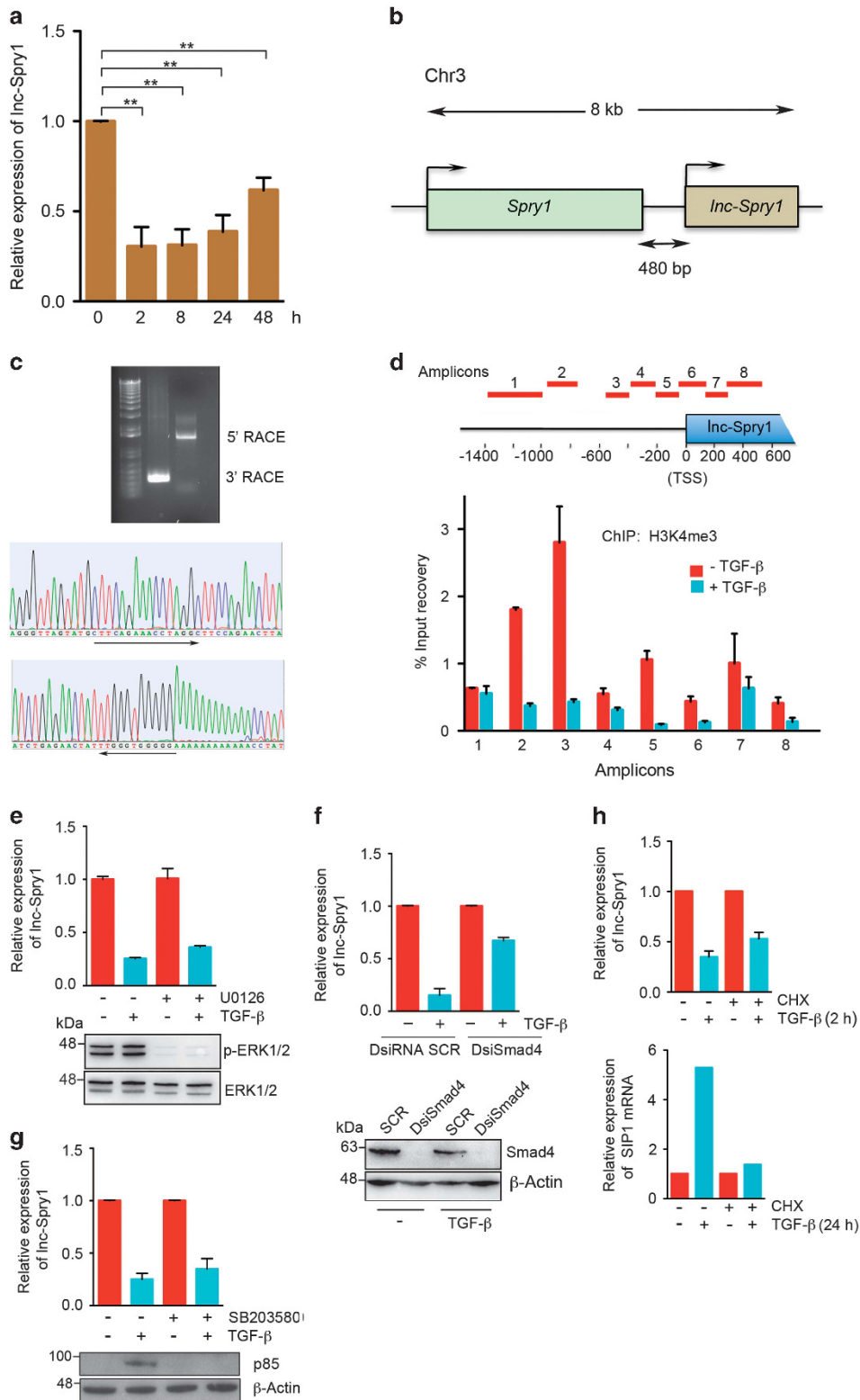


Figure S1e). Six hundred genes were found to be upregulated and 490 downregulated in treated cells compared with untreated cells, including 215 downregulated and 220 upregulated lncRNAs (Supplementary Table S1). Expression of several candidates was confirmed by real-time PCR. Among them, we focused on AK040898 located on mouse chromosome 3, because of its consistent early downregulation (Figure 1a). We termed this candidate lnc-Spry1 based on the name of the neighboring gene.

Given the proximity of lnc-Spry1 to the Spry1 gene (Figure 1b), and the fact that both are transcribed in the same orientation, we sought to ensure that the lnc-Spry1 transcript was distinct from that of the Spry1 gene. We determined by 5' and 3' rapid amplification of cDNA ends (RACE) that lnc-Spry1 is a 2851 nucleotides transcript without introns, 472 nucleotides shorter at the 5' end than the ENCODE AK040898 transcript annotation (Figure 1c and Supplementary Figure S1). We next sought to detect trimethylation of histone H3 at lysine 4 (H3K4me3) enrichment at the 5' regulatory region of lnc-Spry1. Chromatin immunoprecipitation assays showed a remarkable H3K4me3-enriched region within 800 bp of the lnc-Spry1 transcription start site, enrichment not detected in TGF- β -treated cells (Figure 1d). These data indicate that Spry1 mRNA and lnc-Spry1 RNA are transcribed from independent promoters. Sequence analysis using ORF Finder (NCBI) predicted open reading frames <70 amino acids without a valid Kozak sequence. In addition, a low coding potential score (-0.924) and a low coding probability (0.032) returned by the Coding Potential Calculator software²³ and Coding-Potential Assessment Tool,²⁴ respectively, confirmed a negligible protein-coding potential for lnc-Spry1. Sequence homology searches and 5' RACE analysis revealed no clear orthologous lnc-Spry1 sequence or transcripts in syntenic regions of the human genome, suggesting that lnc-Spry1 is a mouse-specific lncRNA. Smad4 is a central mediator of TGF- β intracellular signaling.²⁵ We investigated the requirement of Smad4 in lnc-Spry1 downregulation by TGF- β . Two different commercial Dicer-substrate short interfering RNAs were used for silencing Smad4 and the knockdown efficiencies were tested by western blotting. lnc-Spry1 downregulation by TGF- β treatment was notably affected in Smad4-suppressed

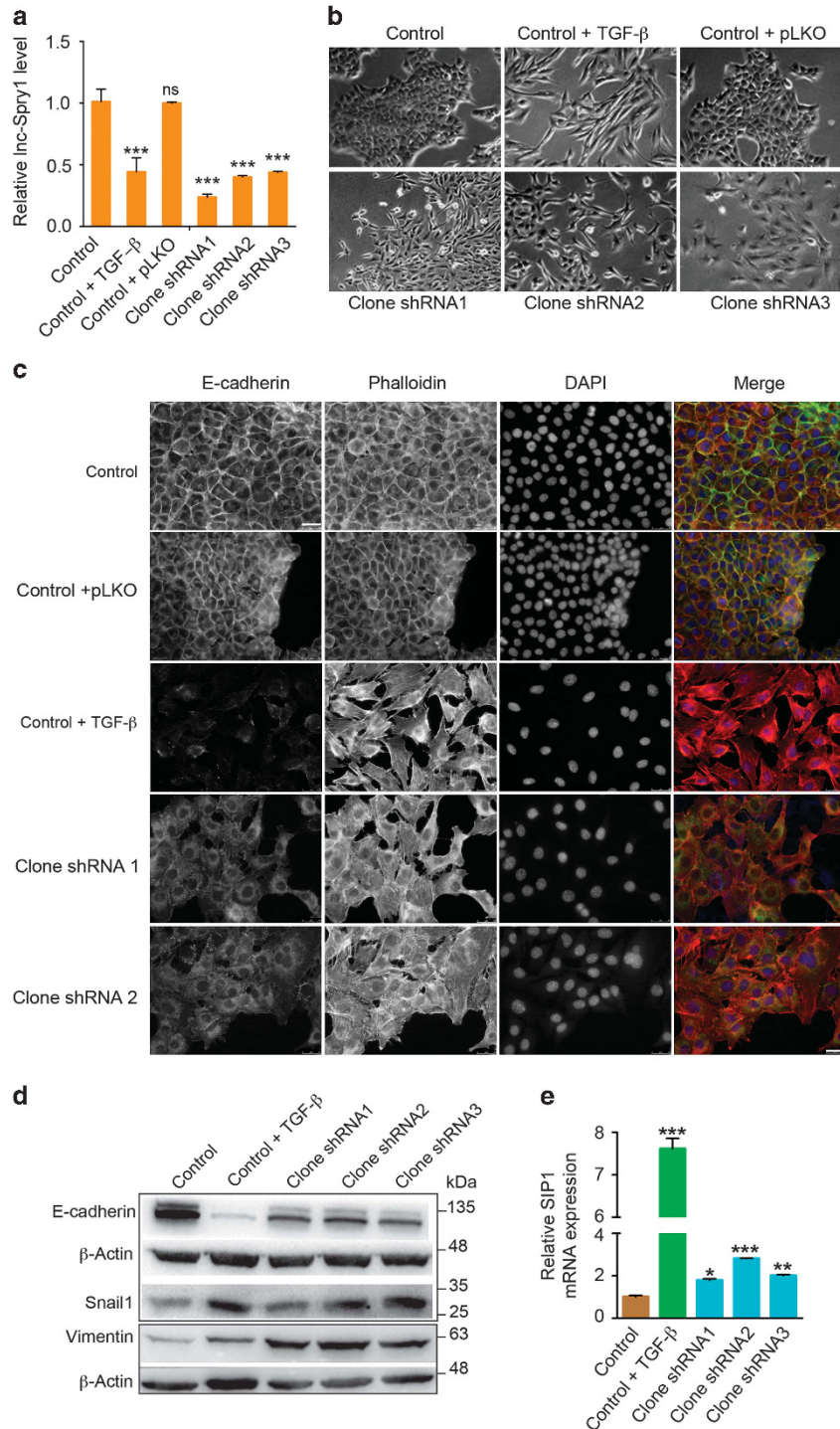
cells, indicating TGF- β -Smad signaling dependency of this TGF- β response (Figure 1f). Smad-mediated signaling pathway, extracellular signal-regulated kinases (ERKs) and p38 kinases are activated very rapidly in TGF- β -treated NMuMG cells.²⁶ However, lnc-Spry1 downregulation appeared to uniquely rely on the Smad-mediated pathway, as preincubation of NMuMG cells with the MEK inhibitor U0126 and the p38 inhibitor SB203580 had no effect on TGF- β -downregulated lnc-Spry1 (Figures 1e and g). lnc-Spry1 downregulation detected within 15 min of TGF- β treatment (Figure 4b) suggested an active role in the start of EMT program. To determine whether lnc-Spry1 was a direct target of TGF- β -Smad pathway, we analyzed the levels of lnc-Spry1 in cells treated with TGF- β in the presence or absence of cycloheximide, an inhibitor of protein synthesis. Cycloheximide treatment did not inhibit downregulation of lnc-Spry1, whereas upregulation of SIP1, an indirect target control of the TGF- β -Smad pathway,²⁷ was blocked (Figure 1h). Together, these findings strongly suggest that lnc-Spry1 is downregulated by TGF- β -Smad signaling and it is a direct target of this pathway.

lnc-Spry1 downregulation promotes a mesenchymal-like phenotype. To investigate whether the reduced expression of lnc-Spry1 could promote the process of EMT, we generated short hairpin RNAs (shRNA)-mediated knockdown stable clones using three lnc-Spry1-targeting shRNA expression constructs. Expression of lnc-Spry1 was reduced from 60 to 70% using these different shRNAs (Figure 2a). A consistent epithelial-to-mesenchymal-like phenotype was observed for all three shRNAs used (Figure 2b), indicating that this change was specific and was not likely due to off-targeting. Furthermore, immunofluorescence analysis revealed a decrease in the epithelial marker E-cadherin expression and the remaining protein was dislocated from the membrane to the cytoplasm. In the absence of TGF- β , phalloidin-labeled F-actin was predominantly organized in thin cortical bundles tightly associated with cell-cell adhesions.²⁸ In contrast, after 48 h of treatment with TGF- β , F-actin was assembled into thick parallel bundles, or actin stress fibers, traversing the ventral cell surface. We also observed a notable remodelling of the cytoskeleton from cortical actin to stress fibers in lnc-Spry1-depleted cells

Figure 1 lnc-Spry1 expression in TGF- β -treated NMuMG cells. (a) Expression of lnc-Spry1 measured by quantitative reverse transcriptase-PCR (RT-qPCR) at representative time points shows decreased levels in TGF- β -treated cells. Experiments were performed in triplicate, and error bars represent S.D. ** $P < 0.01$ by two-tailed Student's *t*-test. (b) Schematic illustration of the mouse lnc-Spry1 gene locus chromosomal location. Arrowheads indicate the transcription orientation. (c) Top, a representative image of PCR products from the 5'-RACE and 3'-RACE procedure. Bottom, sequencing of PCR products revealed the boundary between the adaptor primers and lnc-Spry1 sequences. (d) Chromatin immunoprecipitation analysis were performed to study H3K4me3 enrichment at the lnc-Spry1 5' regulatory region of NMuMG control cells and NMuMG stimulated with TGF- β for 2 h. Transcription start site (TSS) and the enrichment regions analyzed are indicated in the figure. Enrichment values are represented as the percentage of recovered input. Control cell data are the mean of at least $n = 9$ qPCR reactions from three independent experiments. Background enrichment with normal rabbit IgG was <0.05% of the total input chromatin. TGF- β -treated cell data are the mean of $n = 6$ qPCR reactions from two independent experiments. Background enrichment with normal rabbit IgG was <0.015% of the total input chromatin. (e) Effect of MAP kinase inhibitor, U0126, on lnc-Spry1 downregulation. NMuMG cells were pretreated with 10 μ M inhibitor for 1 h prior to addition of TGF- β for 2 h where indicated. lnc-Spry1 levels were measured by RT-qPCR (top); p-ERK1/2 were assessed by western blotting and total ERK1/2 were used as protein loading control (bottom). (f) NMuMG cells were transfected with DsiRNAs against Smad4 (DsiSmad4) or scramble DsiRNA (SRC) and treated with TGF- β for 2 h. Levels of lnc-Spry1 were measured by RT-qPCR analysis (top). Smad4 was assessed by western blotting (bottom); β -actin was used as protein loading control. (g) Effect of p38 kinase inhibitor, SB203580, on lnc-Spry1 downregulation. Cells were pretreated with 10 μ M inhibitor for 1 h prior to addition of TGF- β for 2 h where indicated. Levels of lnc-Spry1 were measured by RT-qPCR analysis (top). Activation of p38 kinase was detected via phosphorylated p85 ribosomal kinase (p85). A representative immunoblot analysis for p85 is shown (bottom); β -actin was used as a protein loading control. (h) Requirement of *de novo* protein synthesis for lnc-Spry1 downregulation by TGF- β . NMuMG cells pretreated with 5 μ M of cycloheximide (CHX) for 1 h were stimulated with TGF- β for 2 h (top) or 24 h (bottom). Expression levels of lnc-Spry1 (top) and SIP1 (bottom) were measured by RT-qPCR analysis

(Figure 2c). Immunoblotting analysis revealed a remarkable increase in the expression of mesenchymal markers, such as vimentin and Snail1, and a decrease in the expression of the epithelial marker E-cadherin in Lnc-Spry1-depleted clones compared with control clones (Figure 2d). Also RT-qPCR analysis showed that mesenchymal marker SIP1 was slightly increased in Lnc-Spry1-depleted clones (Figure 2e). As Lnc-Spry downregulation mimics TGF- β signaling in terms

of EMT induction, we wondered whether Lnc-Spry1 downregulation induced TGF- β expression and this could cause an autocrine TGF- β signaling. Quantification of TGF- β mRNA levels in Lnc-Spry1-depleted shRNA1 and shRNA2 clonal cell lines showed that these clones contained TGF- β mRNA levels 1.4 and 2.2 times higher, respectively, than control cells. To test a possible role of autocrine TGF- β signaling in Lnc-Spry1-depleted clones, we treated them with TGF- β type I receptor



(ALK5) kinase inhibitor SB431542.²⁹ Clones were minimally affected by treatment with the inhibitor and showed mesenchymal-like phenotype (Supplementary Figure S2a), and EMT-related molecules analyzed were not significantly affected (Supplementary Figures S2b–e). These results indicate that downregulation of *lnc-Spry1* promotes *per se* a mesenchymal-like phenotype. As cell migration and invasion are altered in EMT, we assessed the migratory capacity and invasiveness of *lnc-Spry1*-silenced cells. Wound-healing assays revealed that sh*lnc-Spry1* NMuMG cells migrated much faster than control cells (Figures 3a–c and Supplementary Movie S1). Furthermore, the effect of *lnc-Spry1* downregulation on cell invasion was determined in invasion assays in matrigel-coated transwell chambers. *lnc-Spry1* silencing resulted in a highly significant increase in the invasive potential of NMuMG cells (Figures 3d and e). However, monitoring of NMuMG real-time cell proliferation showed no differences between control and *lnc-Spry1*-depleted cells (Figure 3f). These results demonstrate a role of *lnc-Spry1* in remodeling the cell cytoskeleton and the effect of its depletion on cell migration and invasion.

Lnc-Spry1 depletion alters gene expression. LncRNAs have been shown to regulate the expression of neighboring genes in *cis* or in *trans* by diverse mechanisms.³⁰ The *Spry1* gene is located 480 bp upstream from *lnc-Spry1* and, therefore, could be a candidate to be regulated in *cis*. In fact, *lnc-Spry1*-depleted clones markedly reduced the *Spry1* mRNA levels (Figure 4a). This effect was specific for *Spry1* gene, as changes were not detected in other protein-coding genes surrounding *lnc-Spry1* (Supplementary Figure S3). A detailed time course of *lnc-Spry1* and *Spry1* mRNA expression after TGF- β treatment for short periods of time showed a strong correlation between downregulation of both genes (Figure 4b). Similar to the effect of cycloheximide on *lnc-Spry1* downregulation in TGF- β -treated cells, downregulation of *Spry1* mRNA levels was not affected by cycloheximide, indicating that *Spry1* is a direct target (Figure 4c). Moreover, forced expression of *lnc-Spry1* in *lnc-Spry1*-depleted cells did not rescue the expression of *Spry1* gene (Figures 4d and e), as would be expected from a lncRNA whose primary function was exerted locally.³¹ Also, overexpression of *Spry1* did not lead to any noticeable morphological change in *lnc-Spry1*-depleted cells (Supplementary Figure S4). To determine whether the expression of *lnc-Spry1* and *Spry1* genes were linked, we examined their relative expression across the

same panel of different mouse tissues (Figure 4f). *Spry1* mRNA was found to be much more highly expressed than *lnc-Spry1* in all the tissues analyzed. Both RNAs were more abundant in the heart, lung and muscle. Despite the variation in the expression levels of both transcripts and the different expression in the tissues analyzed, the expression profiles of *Spry1* and *lnc-Spry1* genes were closely correlated (Pearson correlation coefficient $R=0.98$). Altogether, we might suggest that *lnc-Spry1* could act locally to regulate the *Spry1* expression and that they both could regulate similar biological processes. Overexpression of *lnc-Spry1* did not seem to perturb normal EMT by TGF- β . Immunofluorescence analysis of TGF- β -treated control cells and TGF- β -treated *lnc-Spry1*-overexpressing cells did not reveal apparent morphological changes. Also, immunoblot analysis of E-cadherin, vimentin, Snail1 and *Spry1* proteins did not show any significant change in the expression levels of these proteins (Supplementary Figure S5). This result would be consistent with the fact that EMT relies on a complex signaling network that involves multiple transcription factors and signaling proteins, in some instances, with redundant functions. As Snail1 transcription factor is a major regulator of EMT and it is a primary responder to TGF- β treatment,^{32,33} we tested whether ectopic expression of Snail1 affected the levels of *lnc-Spry1* and *Spry1* mRNA. Expression of both genes was unaffected by overexpression of Snail1, indicating that Snail1 is not required for *lnc-Spry1* inhibition upon TGF- β treatment (Supplementary Figure S6). We next reasoned that analysis of global gene expression pattern in *lnc-Spry1*-depleted cells could reveal further clues toward elucidating its function. Changes in RNA levels were analyzed by DNA microarray analysis both in stable *lnc-Spry1*-depleted cells and control cells. We found 181 misregulated genes in the *lnc-Spry1*-depleted cells (lineal change >2-fold and P -value <0.05) among which 110 were downregulated and 71 were upregulated (Figure 4g and Supplementary Table S2). RT-qPCR analysis confirmed microarray results for 10 of the 12 selected genes (83%), including downregulation of *Id2*, *Sim2*, *Atoh8*, *Cxcl5*, *Ccl20* and upregulation of *Sox9* (Supplementary Figure S7). Gene ontology analysis of misregulated genes in *lnc-Spry1*-depleted cells showed a notable enrichment in those genes involved in chemokine and cytokine activity (*Ccl2*, *Ccl20*, *Ccl7*, *Cxcl1*, *Cxcl16*, *Bmp2*, *Grem1*) (Figure 4h). Strikingly, 30 and 28% of downregulated and upregulated genes, respectively, were also downregulated and upregulated in TGF- β treated

Figure 2 Downregulation of *lnc-Spry1* promotes a mesenchymal-like phenotype. (a) *lnc-Spry1*-downregulated cell lines were generated by transduction of shRNA expression lentivirus against either *lnc-Spry1* or a non-targeting control. *lnc-Spry1* RNA levels were determined by quantitative reverse transcriptase-PCR (RT-qPCR) in NMuMG cells treated with TGF- β for 48 h, in a clonal cell line transduced by empty lentivirus (pLKO), three clonal cell lines expressing reduced levels of *lnc-Spry1* and a control cell line. Experiments were performed in triplicate, and error bars represent S.D. within one representative experiment. Results were analyzed by one-way analysis of variance, followed by Bonferroni posttest. *** $P < 0.001$, NS, not significant. (b) Downregulation of *lnc-Spry1* induces morphological changes in NMuMG cells. Phase-contrast images illustrate that cells depleted of *lnc-Spry1* undergo EMT-like changes in morphology, including a reduction in cell–cell contacts and cobblestone appearance. (c) Immunofluorescence microscopic analysis of changes in location and the expression of marker proteins. Cells were stained with antibodies against the epithelial marker E-cadherin and with tetramethylrhodamine isothiocyanate (TRITC)-conjugated phalloidin and 4,6-diamidino-2-phenylindole to visualize the actin cytoskeleton and nuclei, respectively. Scale bar, 25 μ m. (d) Immunoblotting of Snail1, E-cadherin and vimentin in NMuMG cells, NMuMG treated with TGF- β for 48 h and *lnc-Spry1*-downregulated NMuMG clones generated by transduction of shRNAs expression lentivirus against *lnc-Spry1*. β -Actin was used as a loading control. (e) Expression levels of *SIP1* mRNA were determined by RT-qPCR in NMuMG control cells, treated with TGF- β for 48 h and three clonal cell lines expressing reduced levels of *lnc-Spry1*. Error bars represent S.D. *** $P < 0.001$, ** $P < 0.01$, * $P < 0.05$ by two-tailed Student's t -test

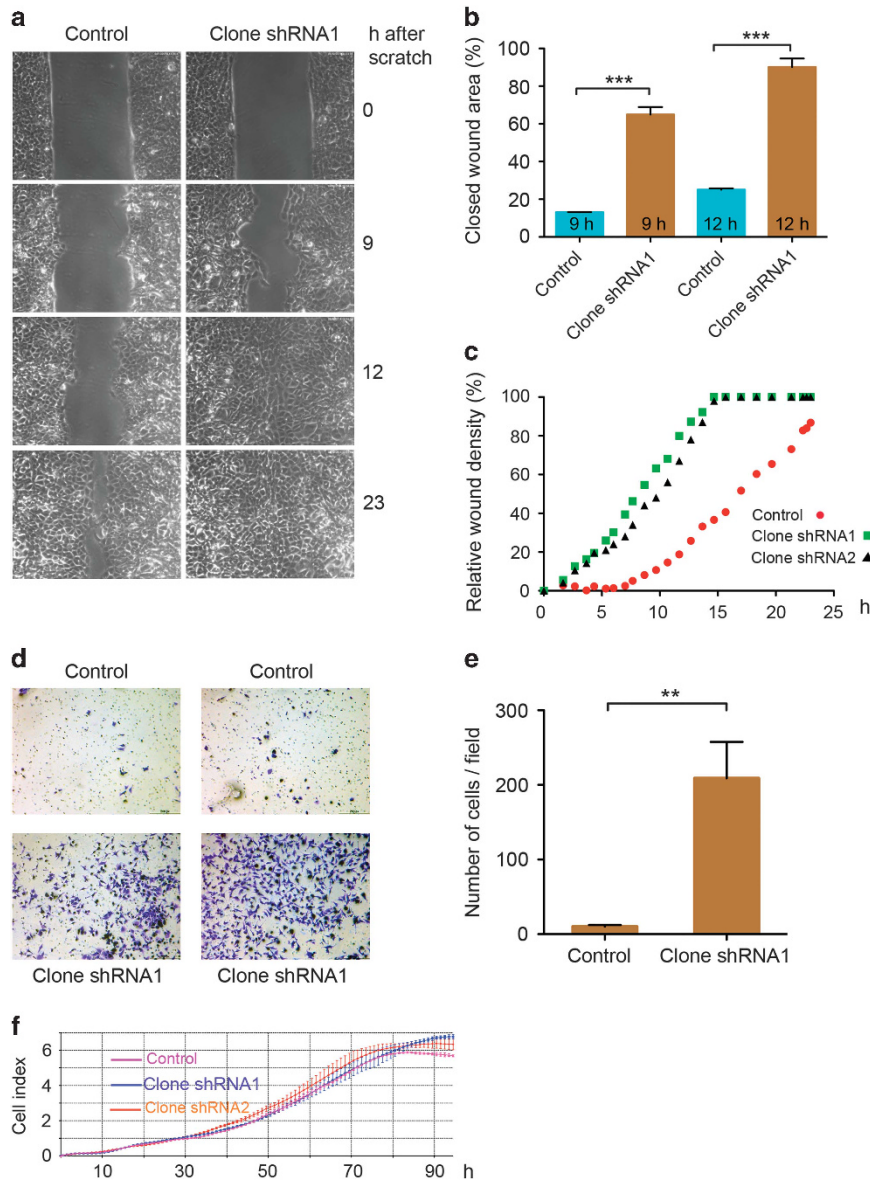


Figure 3 Lnc-Spry1-depleted cells acquire migratory and invasive properties. (a) The migratory capacity of Lnc-Spry1-downregulated NMuMG cells were tested in wound-healing assays. Cells were imaged at 20 min intervals for 23 h. The frames of the movie at 9, 12 and 23 h are shown. (b) The frames at 9 and 12 h are used to estimate the percentage of surface covered by the cells. Values represent the average (%) of wound closure \pm S.E. *** $P < 0.001$ by two-tailed Student's *t*-test. (c) Wound density quantitation of the time-lapse video frames from control and two Lnc-Spry1-depleted clonal cell lines. (d) Representative images of invasion in a clonal cell line expressing reduced levels of Lnc-Spry1 and in a control cell line analyzed in a transwell invasion assay. After 24 h, cells were fixed and stained with crystal violet. (e) Histograms represent the mean \pm S.D. of the number of cells per field counted in three different inserts. ** $P < 0.01$ by two-tailed Student's *t*-test. (f) Real-time monitoring of *in vitro* proliferation of two clonal cell lines expressing reduced levels of Lnc-Spry1 and a control cell line using the eCELLigence system. The system measures electrical impedance across interdigitated microelectrodes integrated on the bottom of tissue culture plates

cells (Figure 4i and Supplementary Table S3) (P -value = 4.7×10^{-48} and P -value = 6.9×10^{-20} , hypergeometric distribution), strongly suggesting that Lnc-Spry1 could participate directly and indirectly in TGF- β -dependent transcriptional response.

Lnc-Spry1 interacts with the U2AF65 spliceosome component. To investigate the mechanism by which Lnc-Spry1 mediates gene regulation, we searched for proteins that were associated with Lnc-Spry1 using *in vitro* biotin-RNA

pull-down. *In vitro*-transcribed biotinylated Lnc-Spry1 and a non-relevant RNA as a negative control were incubated with total cellular extracts and coprecipitated proteins were isolated using streptavidin-coated beads. RNA-associated proteins were resolved on a SDS-PAGE gel, and specific bands to the Lnc-Spry1 probe were visualized using SYPRO Ruby staining and cut out for analysis by mass spectrometry (Figure 5a), identifying U2AF65 as a protein specifically associated with Lnc-Spry1 (Supplementary Figure S8). These interactions were confirmed by western blotting analysis

(Figure 5b) and RNA immunoprecipitation (RIP). Enrichment of Inc-Spry1 RNA was observed using specific U2AF65 antibody

compared with non-specific IgG antibody (Figure 5c). Additionally, deletion-mapping experiments combined with western blotting analysis showed that the different truncated

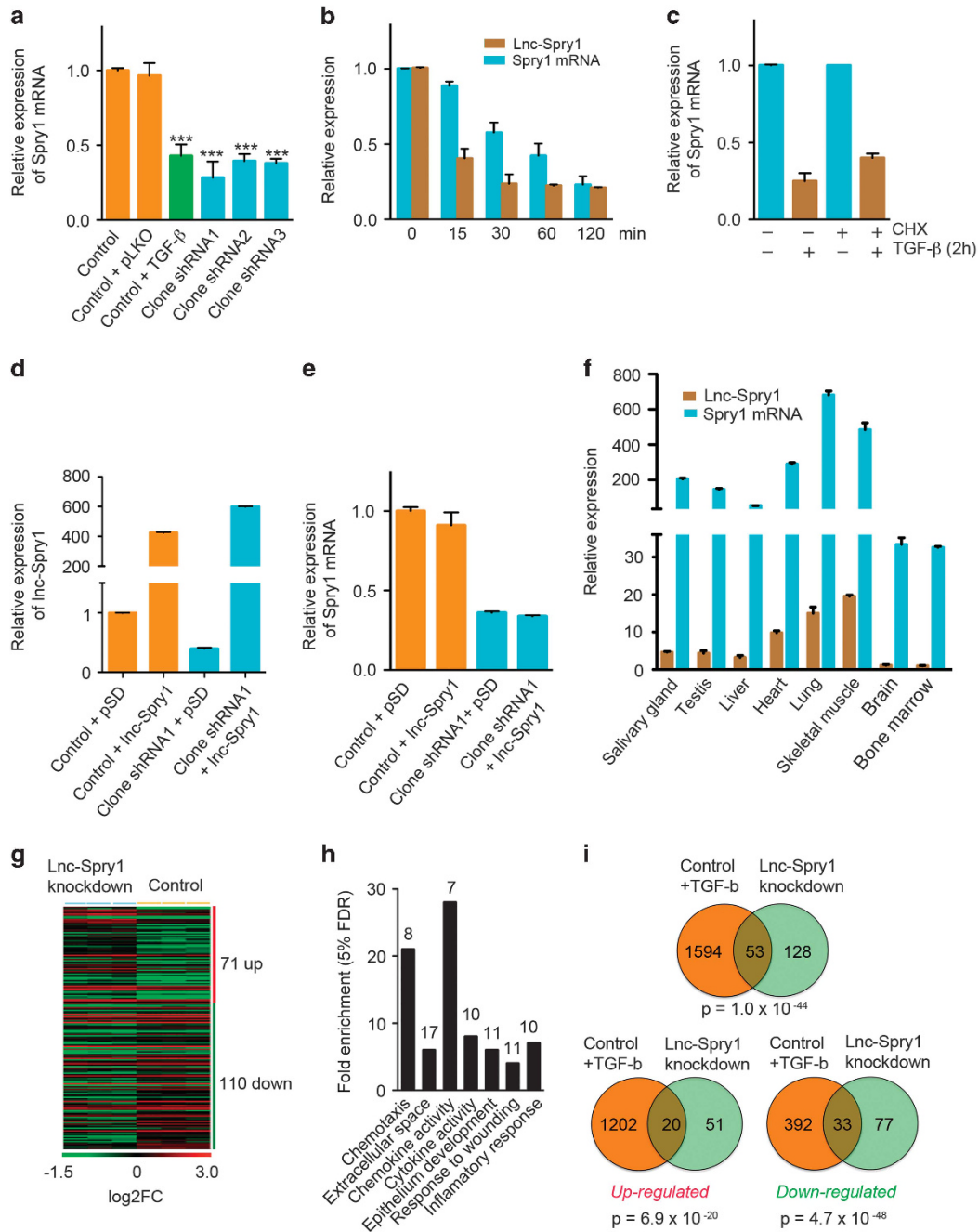


Figure 4 Gene expression is affected in Inc-Spry1-depleted cells. (a) Relative Spry1 mRNA levels determined by quantitative reverse transcriptase-PCR (RT-qPCR) in control cells, clonal cell line transduced by empty lentivirus (pLKO), cells treated with TGF-β for 48 h and three independent shRNA-mediated knockdown of Inc-Spry1 stable clones. Results were analyzed by one-way analysis of variance, followed by Bonferroni posttest. ***P < 0.001. (b) Relative Inc-Spry1 and Spry1 mRNA levels determined by RT-qPCR in NMuMG control cells treated with TGF-β for 15, 30, 60 and 120 min. Error bars represent S.D. (c) Expression levels of Spry1 mRNA in NMuMG cells pretreated with 5 μM cycloheximide (CHX) for 1 h and stimulated with TGF-β for 2 h. (d) Real-time PCR analysis of Inc-Spry1 levels in cells infected at MOI 2 with pHRIS-DUAL lentivirus control (pSD) or lentivirus carrying full-length Inc-Spry1 cDNA. Error bars represent S.D. within one representative experiment. (e) Relative levels of Spry1 mRNA in cells overexpressing Inc-Spry1. (f) Relative Inc-Spry1 and Spry1 mRNA levels determined by RT-qPCR in a broad range of adult mouse tissues. Results are presented relative to the average value of HPRT reference gene and a fixed reference sample (bone marrow). (g) Heat map showing statistically significant changes of 181 genes in Inc-Spry1-depleted cells. Color intensities are shown on a log₂ scale. (h) Significant Gene Ontology annotation enrichments of Inc-Spry1-regulated genes (5% FDR). (i) Venn diagram showing the intersection of genes affected in TGF-β-treated or Inc-Spry1-depleted cells. All misregulated genes in the upper panel. Lower left and right panels: upregulated and downregulated genes, respectively. Probability of overlapping based on hypergeometric distribution is provided

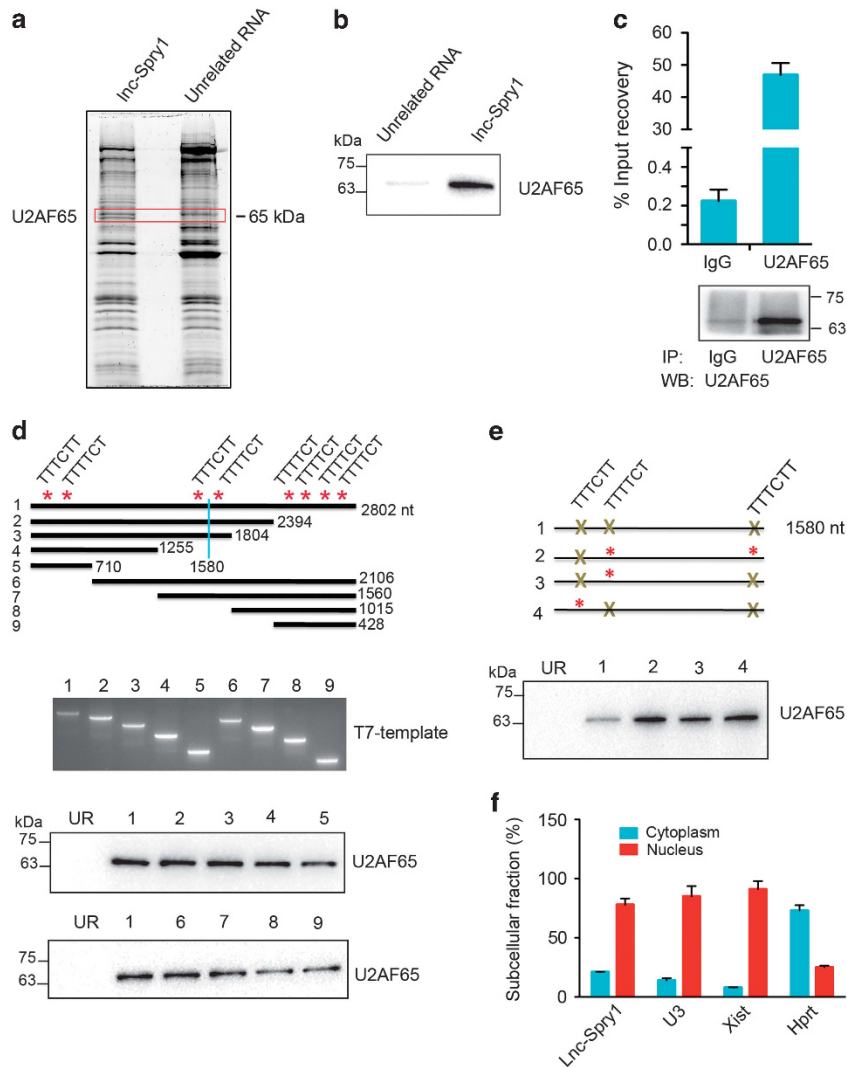


Figure 5 Lnc-Spry1 interacts with U2AF65 splicing factor. (a) A representative Sypro ruby-stained gel picture showing the proteins bound to Lnc-Spry1 (left lane) or unrelated RNA (right lane). The highlighted region was analyzed by mass spectrometry. U2AF65 was identified as Lnc-Spry1-binding partner. (b) Western blotting analysis of the specific interaction between U2AF65 and Lnc-Spry1. Protein loading normalization was performed by measuring total protein directly on the membrane using the criterion stain-free gel imaging system. (c) Physical association of Lnc-Spry1 and U2AF65 determined by RNA immunoprecipitation (RIP). (Bottom) Representative western blotting of U2AF in the corresponding samples. Results are the median of three technical replicates; bars represent S.D. (d) Deletion analysis of Lnc-Spry1 transcript. Motifs for U2AF65 binding in Lnc-Spry1 are shown. Associated U2AF65 with different RNA fragments was detected by western blotting. (e) Associated U2AF65 with the 1580 nt Lnc-Spry1 fragment after mutagenesis of U2AF65-binding sites. (f) Lnc-Spry1 subcellular localization. Expression of Lnc-Spry1, U3, Xist and Hprt in nuclear and cytoplasmic fractions of NMuMG cells. Error bars represent S.D.

versions of Lnc-Spry1 associated with U2AF65. Lnc-Spry1 sequence contained several disseminated U2AF65-binding sites (Figure 5d) and association between U2AF65 and Lnc-Spry1 decreased drastically after mutagenesis of some of these binding sites (Figure 5e). Next, Lnc-Spry1 expression was measured in nuclear and cytosolic fractions from NMuMG cells by RT-qPCR. The differential enrichments of HPRT, Xist and U3 RNAs were used as fractionation indicators. A considerable increase in Lnc-Spry1 level was observed in the nucleus of NMuMG cells (Figure 5f), indicating that Lnc-Spry1 may have a major regulatory function.

Lnc-Spry1 modulates EMT-associated AS. A strong link between EMT and AS has been demonstrated in the case of

FGF receptors (FGFRs). A functional FGFR consists of three extracellular immunoglobulin domains (Ig-I, Ig-II and Ig-III), a single-transmembrane domain, and a cytoplasmic tyrosine kinase domain. AS in the second half of the third extracellular immunoglobulin-like domain is encoded by one of the two mutually exclusive alternative exons: IIIb or IIIc. The expression of either isoform is highly cell-type specific, with FGFR2IIIb expression predominantly expressed in epithelial cells and FGFR1IIIc and FGFR2IIIc mainly expressed in mesenchymal cells. Given the interaction between U2AF65 and Lnc-Spry1 and the documented role of U2AF65 in splicing regulation, we hypothesized that Lnc-Spry1 could have a *trans*-mediated effect in AS by leading or fitting the pool of U2AF65. Analysis by RT-qPCR of FGFR1 and FGFR2 mRNA levels showed that FGFR1 mRNA levels increased 60-fold in

cells stimulated with TGF- β for 48 h and from 11- to 20-fold in lnc-Spry1-depleted cells, whereas FGFR2 mRNA levels decreased in both conditions (Figures 6a and b). Using

isoform-specific primers, we determined that the FGFR1 isoform upregulated by TGF- β or by lnc-Spry1 depletion was the mesenchymal isoform FGFR1IIIc (Figure 6c), whereas

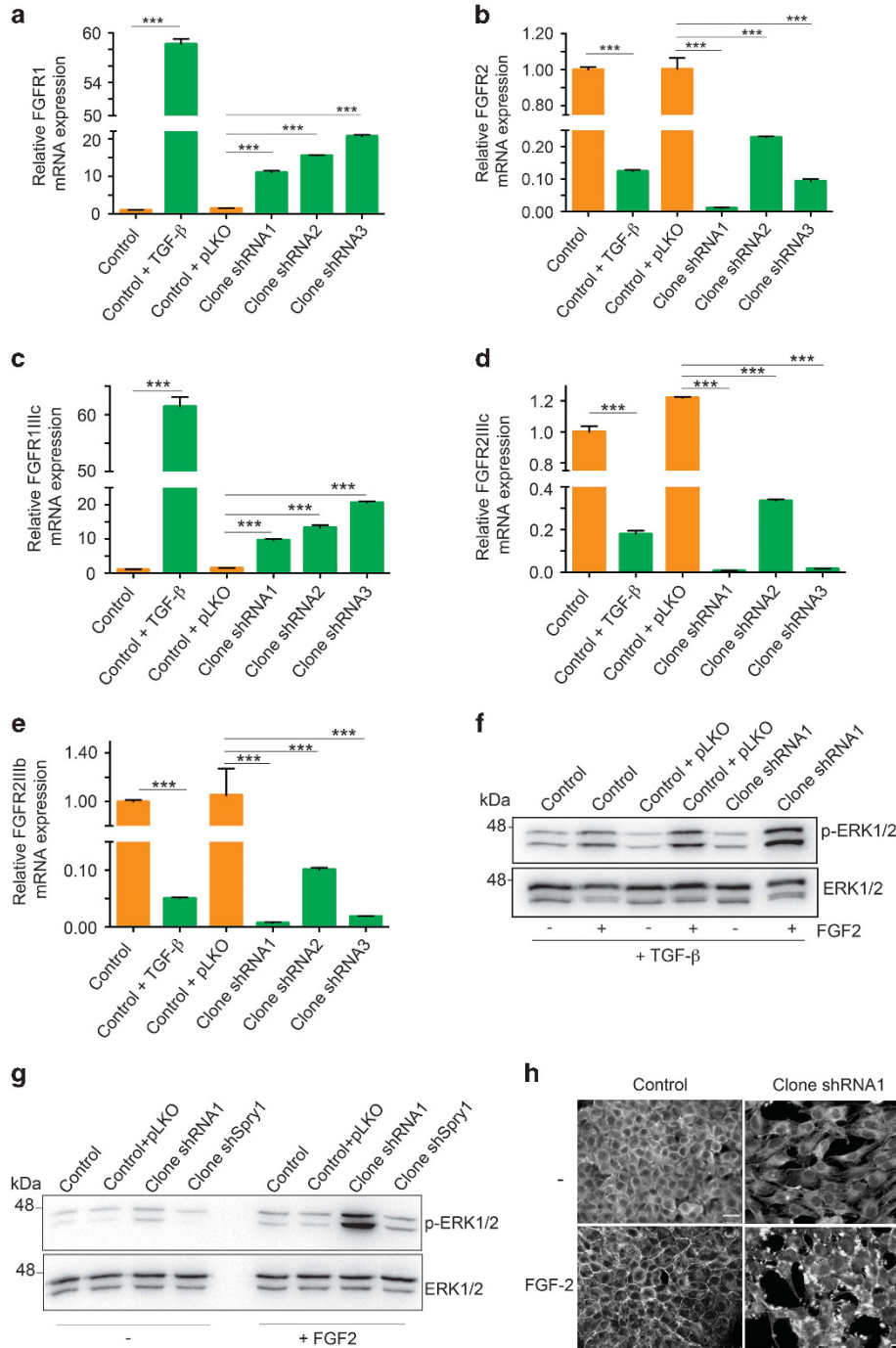


Figure 6 Isoform switching of FGFRs in TGF- β -treated cells and lnc-Spry1-depleted cells. (a and b) Expression levels of FGFR1 and FGFR2 in NMuMG control cells, treated with TGF- β for 48 h, a clonal cell line transduced by empty lentivirus (pLKO) and three clonal cell lines expressing reduced levels of lnc-Spry1. Error bars represent S.D. *** P < 0.001 by two-tailed Student's t -test. (c–e) Expression of the alternatively spliced forms of FGFR1 and FGFR2 in NMuMG control cells, treated with TGF- β for 48 h, in a clonal cell line transduced by empty lentivirus (pLKO) and in three clonal cell lines expressing reduced levels of lnc-Spry1. Error bars represent S.D. *** P < 0.001 by two-tailed Student's t -test. (f and g) Representative western blotting results for ERK1/2 and p-ERK1/2 protein expression from NMuMG control cells, a clonal cell line transduced by empty lentivirus (pLKO) and a clonal cell line expressing reduced levels of lnc-Spry1 (Clone shRNA1). NMuMG cells were preincubated with (f) or without (g) TGF- β for 2 days and then stimulated with 30 ng/ml FGF-2 for 15 min. A clonal cell line expressing reduced levels of Spry1 mRNA (Clone shSpry1) is included in panel (g). (h) Immunofluorescence analysis of actin cytoskeleton reorganization in NMuMG control and lnc-Spry1-depleted cells cultured in the presence of 30 ng/ml FGF-2 for 48 h. Scale bar, 25 μ m

both FGFR2IIlc and FGFR2IIlb isoforms were downregulated (Figures 6d and e). The different isoforms generated by this splicing event show distinct FGF-binding specificities. During TGF- β -mediated EMT, TGF- β induces isoform switching of FGFRs, sensitizing cells to FGF-2, which binds preferentially to IIlc isoforms, whereas FGF-7 and FGF-10 bind exclusively to IIlb isoforms.³⁴ As shown in Figure 6f, addition of FGF-2 to TGF- β -treated cells induced ERK signaling pathway, revealing isoform switching by TGF- β treatment. Interestingly, addition of FGF-2 activated ERK signaling pathway in Lnc-Spry1-depleted cells without previous TGF- β treatment (Figure 6g). ERK phosphorylation was not observed in Spry1-depleted cells, which showed reduced levels of FGFR1IIlc, FGFR2IIlb and FGFR2IIlc (Figure 6g and Supplementary Figures S10b–d). Likewise, morphology of Spry1-depleted cells was not affected after FGF-2 addition (Supplementary Figure S10e), whereas Lnc-Spry1-depleted cells showed a dramatic accumulation of the actin cytoskeleton into large clumps (Figure 6h), supporting a role for Lnc-Spry1 in modulating the stability of actin cytoskeletal structures. Epithelial Splicing Regulatory Proteins 1 and 2 (ESRP1 and ESRP2) are key epithelial-specific RNA-binding proteins that promote splicing of the epithelial variant of the FGFR transcripts. In NMuMG cells, induction of EMT by TGF- β is accompanied by nearly complete abrogation of ESRP2 expression (ESRP1 is not expressed in NMuMG cells) and consequent isoform switching of FGFRs.^{12,35} Strikingly, depletion of Lnc-Spry1 mimics the effects of TGF- β on FGFRs splicing; however, ESRP2 protein levels are not affected in Lnc-Spry1-depleted cells (Supplementary Figure S9). This fact together with the clear evidence of interaction between Lnc-Spry1 and U2AF65 may suggest a redundant mechanism for FGFR isoform switching.

Discussion

The precise regulation of gene expression patterns is paramount in the transdifferentiation of epithelial cells into mesenchymal cells.^{36,37} LncRNAs have emerged as key regulatory components in different processes.^{14,16,38,39} Several lncRNAs have been analyzed and associated with EMT in cells upon TGF- β treatment for one or several days.^{21,40,41} We hypothesized that lncRNAs could have an essential role as early master regulators during EMT. Here Lnc-Spry1 is identified as an immediate-early gene downregulated by TGF- β with potential implications in EMT. According to ENCODE genomic annotations, 5' end of Lnc-Spry1 is 10 nucleotides away from 3' end of Spry1 gene and both genes are located in the same DNA strand and show the same orientation, supporting the hypothesis that Lnc-Spry1 could be an extension of the protein-coding Spry1 transcript. However, experiments of RACE and TGF- β -dependent enrichment of active promoter tags around the transcription start site rule out the presence of a long Spry1 isoform containing Lnc-Spry1 as an extended 3' UTR and support that Spry1 and Lnc-Spry1 exist as two independent RNAs.

Signaling through TGF- β receptor complexes involves SMAD-dependent and SMAD-independent pathways.⁴² In NMuMG cells stimulated with TGF- β , we found activation at short time of both ERK and p38 kinases; however, the

presence of specific inhibitors of MEK and p38 MAPK kinases did not affect Lnc-Spry1 downregulation. In contrast, it was notably affected in SMAD4-depleted cells. Downregulation of Lnc-Spry1 was detected as early as 15 min poststimulation with TGF- β , and it was also observed in cells pretreated with cycloheximide demonstrating that it did not require *de novo* protein synthesis and could be categorized as an immediate-early response gene and a direct target of TGF- β -Smad pathways in NMuMG cells.

Knockdown and ectopic expression of multiple lncRNAs reveal their influence on the transcription of their neighboring protein-coding genes.^{43,44} In line with these observations, some findings suggest a local regulation of Spry1 gene by Lnc-Spry1, such as close vicinity of Spry1 to Lnc-Spry1, concurrent, rapid and *de novo* protein synthesis-independent downregulation of both genes in TGF- β -treated cells, downregulation of Spry1 in Lnc-Spry1-depleted cells, close correlation between Lnc-Spry1 and Spry1 expression in different organs and tissues and failure to rescue Spry1 expression in Lnc-Spry1-depleted cells after forced expression of Lnc-Spry1. Spry proteins are feedback regulators of receptor tyrosine kinases (RTKs) that restrain RTK-mediated ERK signaling, and therefore they have critical roles in the regulation of cell proliferation, differentiation and survival,^{45,46} and its downregulation could contribute to mesenchymal-like phenotype.⁴⁷ Analysis of the protein-coding genes in the 500 kb window surrounding the Lnc-Spry1 did not reveal any transcriptional effect in the neighboring genes, except for Spry1 mRNA; interestingly, forced expression of Spry1 gene did not rescue the epithelial phenotype in Lnc-Spry1-depleted cells. These observations indicated that mesenchymal-like phenotype of Lnc-Spry1-depleted cells seems not to be related only to the action of Lnc-Spry1 on local environment but also it could be a result of *trans*-mediated effects of the Lnc-Spry1 transcript. In association with specific chromatin-modifying complexes, Lnc-Spry1 could regulate *in trans* distantly located genes. In fact, Lnc-Spry1-depleted cells showed expression changes in 181 genes, among which 30 and 28% were enriched for downregulated and upregulated genes, respectively, by TGF- β treatment. Some of them, including downregulated Id2, Sim2, Maf2 and Atoh8 or upregulated Sox9 transcription factors, could be involved in regulating specific sets of EMT-associated genes.^{48,49} Our data show that the expression of Snail1, as well as E-cadherin and vimentin markers, change significantly upon depletion of Lnc-Spry1. Ectopic expression of the transcriptional repressor Snail1⁵⁰ did not affect the expression level of Lnc-Spry1, indicating that Lnc-Spry1 could function upstream or independently of the Snail1 signaling pathway. Interaction between Lnc-Spry1 and the U2AF65 spliceosome component together with the enrichment of nuclear fraction in Lnc-Spry1 suggested an active role in AS for Lnc-Spry1. Recently, lncRNAs have been shown to affect AS by different mechanisms, which provides cells with an additional level of complexity to the regulation of gene expression.^{38,51,52} Extensive changes in AS of many mRNAs have been reported in EMT.^{8,12} In the well-characterized family of FGFRs, it has been reported that FGFR1IIlc and FGFR2IIlb, respective isoforms of FGFR1 and FGFR2, are upregulated and downregulated, respectively, by TGF- β , producing NMuMG cells to be sensitive to FGF-2.³⁴ Lnc-Spry1-depleted cells showed

upregulated FGFR1IIIc isoform and downregulated both FGFR2IIIb and FGFR2IIIc isoforms. Consistent with these changes in mRNA expression profiles of FGFR isoforms, Inc-Spry1-depleted cells showed actin accumulation in large clumps and ERK phosphorylation in response to FGF-2, whereas control cells treated with FGF-2 did not exhibit neither morphological changes nor ERK phosphorylation. Among the splicing factors associated with EMT, downregulation of epithelial splicing regulatory proteins (ESRPs) has been reported to promote a cell-type-specific splicing program that results in isoform switching of FGFRs.⁵³ Here Inc-Spry1 is shown to physically associate with the splicing factor U2AF65, and importantly, its depletion, without altering ESRP protein levels, affects isoform switching of FGFR1 and FGFR2, a similar response to that observed in TGF- β -treated cells.^{8,34,35} Taken together, these observations support the proposal that Inc-Spry1 binding to U2AF65 may modulate its function mimicking endogenous transcripts to hijack or redistribute U2AF65 deflecting it from their primary targets. Reduced levels of Inc-Spry1 upon TGF- β treatment might reroute or alter the binding specificity of U2AF65 protein to influence its proper localization. In summary, our data reveal that Inc-Spry1 is an early TGF- β -downregulated lncRNA that acts as a key multifunctional regulator of TGF- β signaling pathways. The immediate-early downregulation of Inc-Spry1 alters the transcriptional and posttranscriptional gene regulation of the epithelial cells promoting a mesenchymal-like phenotype. Exploring early TGF- β -regulated lncRNAs and elucidating the function may point to new mechanisms and components of the EMT pathways as well as potential therapeutic interventions targeting EMT.

Materials and Methods

Cell culture and reagents. NMuMG cells were grown in Dulbecco's modified Eagle's medium supplemented with 10% fetal bovine serum, 2 mM L-glutamine, 50 U/ml penicillin, 50 U/ml streptomycin and 10 μ g/ml insulin at 37 °C in a 5% CO₂-humidified, 95% air incubator. TGF- β was purchased from PeproTech (London, UK). SB-431542, U0126 and SB-203580 were purchased from Selleck Chemicals (Houston, TX, USA).

lncRNA microarray analysis. Total RNA was extracted from cells using TRIzol (Invitrogen, Carlsbad, CA, USA), in accordance with the manufacturer's protocol, and purified by the RNeasy Mini Kit (Qiagen, Hilden, Germany). Total RNA from each sample was quantified and quality assured by NanoDrop ND-1000 (Thermo Fisher Scientific, Waltham, MA, USA). RNA integrity was assessed by standard denaturing agarose gel electrophoresis. Samples preparation and microarray hybridization were performed based on the manufacturer's standard protocols with minor modifications. Briefly, mRNA was purified from total RNA after removal of rRNA (mRNA-ONLY Eukaryotic mRNA Isolation Kit, Epicentre, Madison, WI, USA). Then each sample was amplified and transcribed into fluorescent cRNA along the entire length of the transcripts without 3' bias using a random priming method (Arraystar Flash RNA Labeling Kit, Arraystar, Rockville, MD, USA). The labeled cRNAs were hybridized onto the Mouse LncRNA Array v2.0 (8 \times 60 K, Arraystar). After having washed the slides, the arrays were scanned by the Agilent Scanner G2505C. Agilent Feature Extraction software (version 11.0.1.1) was used to analyze the acquired array images. Quantile normalization and subsequent data processing were performed using the GeneSpring GX v11.5.1 software package (Agilent Technologies, Santa Clara, CA, USA). After quantile normalization of the raw data, lncRNAs and mRNAs that at least one out of the six samples have flags in Present or Marginal ('All Targets Value') were chosen for further data analysis. The microarray contained probes for 31 423 lncRNAs that were designed by Arraystar based on the most authoritative databases (RefSeq, UCSC Known genes, Ensembl and related literature) and 25 376 coding transcripts. Each transcript is represented by a specific exon or splice junction probe, which can identify individual transcript

accurately. Differentially expressed lncRNAs and mRNAs with statistical significance ((fold change) \geq 2.0, *P*-value \leq 0.05) were identified by comparing the normalized expression levels in TGF- β -treated and untreated samples with a paired *t*-test.

Transfections, lentivirus production and infection assays. Transfection of NMuMG cells was performed using Viromer reagent from Lipocalyx, (Halle, Germany) following the protocol recommended by the manufacturer. Percentage of transfected cells was $>$ 90% and it was quantified by co-expression of the GFP reporter gene. Mouse Spry1 expression vector, pCMV-Sport6.1-Spry1, was obtained from the I.M.A.G.E. Consortium (Nottingham, UK) (accession number BC053428). For lentiviral production, 2.8×10^6 HEK293T cells were seeded onto a 10-cm Petri dish and transfected with Lipofectamine 2000 (Life Technologies, Carlsbad, CA, USA) using 15 μ g of the transfer vectors pHR SIN-DUAL or pLKO together with 10 and 5 μ g of the HIV packaging plasmids pCMVDR8.91 and pVSVG, respectively. Lentiviruses were harvested 48 h posttransfection, passed through a 0.45- μ m filter and concentrated by ultracentrifugation at 100 000 \times g for 90 min. Virus particles were resuspended in serum-free DMEM, snap frozen in liquid nitrogen and stored at -80 °C. Titers of pHR SIN-DUAL lentiviral particles were determined by flow cytometry of NMuMG-infected cells, and titers of pLKO.1 lentiviral particles were determined by transduction of NMuMG cells and subsequent evaluation of the number of colony-forming units following puromycin selection. For generation of Inc-Spry1-downregulated cell lines (shRNAs clones), NMuMG cells were infected with pLKO-shRNA lentiviral supernatant containing 4 μ g/ml polybrene and independent clones were isolated by selection in the presence of puromycin (1 μ g/ml) for 2 weeks. Three independent shnc-Spry1 sequences (shRNA1, shRNA2, shRNA3) were cloned into pLKO.1 vector and tested. Clones expressing shRNA1 gave the most effective Inc-Spry1 silencing (60% reduction of lncRNA-Spry1) and were used in most of the experiments. For ectopic expression of Inc-Spry1 or Snail1 full-length cDNAs, NMuMG cells were infected with pHR SIN-DUAL-Inc-Spry1 or pHR SIN-DUAL-Snail1 lentivirus (MOI = 2), respectively. Mouse Inc-Spry1 gene was cloned by PCR using genomic DNA of NMuMG cells. The purified amplified fragment was cloned into pHR SIN-DUAL lentivector. Primers were designed according to RACE results. Mouse Snail1 expression vector was generated from IMAGE clone 5121591 by subcloning into the same lentivector. The dual-promoter lentivector pHR SIN-DUAL (also known as pHR SIN-CSGWdInotI_pUb_Em) was kindly provided by Mary K Collins (Windeyer Institute, London, UK). Oligonucleotide sequences used for cloning are shown in Supplementary Table S4.

RNA interference. RNA duplexes against Smad4 were prepared by IDT (Leuven, Belgium). DsiRNA sequences are shown in Supplementary Table S4. Cells were transfected with RNA duplexes using Viromer reagent from Lipocalyx following the manufacturer's protocol.

Proliferation, migration and invasion assays. For growth curves, cells were harvested and transferred into 16-well E-plates, which contain electrodes integrated into the bottom surfaces of each well to measure cell index based on impedance using the xCELLigence System (Roche, Indianapolis, IN, USA). In all, 100 μ l of cell culture media were first added to each well at 37 °C for 30 min to equilibrate the conductors to the media. Then, 8, 4, 2 and 1 K cells were added per well, and the program was set to make readings every 30 min for 95 h. Cell migration was measured by using Culture-Inserts (IBIDI, Martinsried, Germany). The Culture-Inserts were transferred to six-well plates, and cells were seeded at a density of 7×10^4 /ml in each well of Culture-Inserts and cultured in phenol red-free complete medium. After 24 h of incubation, the Culture-Inserts were removed, and a 400- μ m cell-free gap was created. Cell migration was observed with a Leica DMI6000 inverted microscope (Leica Microsystems, Wetzlar, Germany) equipped with a Hamamatsu ORCA-ER camera (Hamamatsu, Japan) using LEICA N PLAN 10 \times , /20 \times /0.25 objectives and recorded every 20 min for 23 h. Image processing was carried out using the Leica (LAS) and Adobe Photoshop (Adobe Systems, Mountain View, CA, USA) softwares. Quantification of cell surface was performed using the multiwave length cell-scoring module of the Metamorph Offline software, Molecular Devices, Sunnyvale, CA, USA and the WimScratch Wound Healing Module (WIMASIS, Munich, Germany) program. Transwell invasion assays were performed using Transwell chambers (24 well, 8 μ M pore size; Cell Biolabs, San Diego, CA, USA) coated with basement membrane. Cells were allowed to grow to subconfluency and were serum-starved for 24 h. After detachment with trypsin, cells were washed with PBS, resuspended in serum-free medium and 5×10^4 cells were added to the upper chamber. Complete medium was added to the bottom well of the

chamber. The cells that had not migrated were removed from the upper face of the filters using cotton swabs, and the cells that had migrated to the lower face of the filters were fixed with 3.7% formaldehyde, permeabilized with 100% methanol and stained with 0.05% crystal violet. Images of random fields were captured from each membrane and the number of invasive cells was counted. The mean of triplicate assays was used for each experimental condition.

Immunofluorescence microscopy. Cells grown on coverslips were fixed in 4% paraformaldehyde/phosphate-buffered saline at room temperature for 15 min and then permeabilized by incubation in 0.01% Triton X-100 in PBS. After fixation, the coverslips were blocked with 3% BSA in PBS for 45 min and incubated with primary antibody against E-cadherin (6010181, Transduction Laboratories, San José, CA, USA) for 1 h and then incubated with fluorochrome-labeled secondary antibody or phalloidin (R415, Molecular Probes, Eugene, OR, USA) for 1 h at room temperature. The coverslips were counterstained with DAPI and wide-field fluorescence imaging was performed using a Leica DM6000B microscope (Leica Microsystems). Data were processed with Adobe Photoshop CS4 (Adobe Systems).

Western blotting analysis. Protein expression was determined by immunoblotting using the following specific antibodies: polyclonal rabbit antibody against U2AF65 was purchased from Abcam (Cambridge, UK) (ab37530), monoclonal rabbit antibody against Snail1 was obtained from Cell Signaling (Danvers, MA, USA) (C15D3), monoclonal antibody against vimentin and monoclonal antibody against smad4 were acquired from Santa Cruz (Dallas, TX, USA) (sc-32322 and sc-7966), polyclonal rabbit antibody against ERK1/2 was purchased from ThermoFisher Scientific (Waltham, MA, USA) (61–7400) and polyclonal rabbit antibody against phospho-ERK1/2 and monoclonal antibody against phospho-p70 S6 kinase were purchased from Cell Signaling (#9101 and #9206). Proteins levels were normalized to β -actin (Sigma-Aldrich, St. Louis, MO, USA, A1978). Results were visualized and quantified using ChemiDoc MP Imaging system (Bio-Rad, Hercules, CA, USA). Western blotting analysis of the specific association between lnc-Spry1 and U2AF65 was normalized by measuring total protein directly on the membrane using the criterion stain-free gel imaging system (Bio-Rad).

RNA isolation, RT-qPCR and RACE. Total RNA was isolated using the TRIzol reagent according to the manufacturer's instruction (Invitrogen) and was then reverse transcribed using a mix of oligo(dT)₂₀ and random hexamers and SuperScript III reverse transcriptase. Reverse transcription was followed by SYBR Green quantitative PCR using iTaq Universal SYBR Green Supermix (Bio-Rad). RACE was performed using the FirstChoice RLM-RACE Kit (Ambion, Foster City, CA, USA) following the manufacturer's protocol. RT-PCR primer sequences are listed in Supplementary Table S4.

RNA isolation from mouse tissues. Organs from normal C57BL/6 mice were dissected and immediately frozen in liquid nitrogen and stored at -80°C . To isolate RNA, 40–60 mg of frozen tissue specimens were cut in small pieces and transferred to a tube containing 1 ml of TRIzol Reagent (Invitrogen). Next, they were mechanically homogenized using a Pro250 homogenizer (PROScientific, Oxford, CT, USA) and total RNA was extracted according to the manufacturer's instruction.

RNA pull-down of proteins associated with lnc-Spry1 RNA and site-directed mutagenesis. pCR2.1-Topo plasmid (Invitrogen) containing full-length and truncated lnc-Spry1 cDNAs was linearized with restriction enzyme BamHI and purified using the DNA Clean and Concentrator-5 Kit (Zymo Research, Irvine, CA, USA). A 20- μl reaction contained 1.5 μg linearized plasmid DNA, Biotin RNA labeling mix (Roche) and 40U T7 RNA polymerase (ThermoFisher Scientific) was incubated at 37 $^{\circ}\text{C}$ for 3 h followed by RNase-free DNase I treatment at 37 $^{\circ}\text{C}$ for 30 min. Labeled RNAs were purified using the RNeasy Mini Kit (Qiagen), checked on agarose gel and quantified. Cellular extracts were prepared resuspending 5×10^7 NMuMG cells in 4 ml RIP buffer (25 mM Tris-HCl pH 7.4, 150 mM KCl, 0.5 mM dithiothreitol (DTT), 0.5% NP40, 1 mM PMSF, protease inhibitor cocktail (Roche) and 20 U/ml Rnasin ribonuclease inhibitor (Promega, Madison, WI, USA) and incubated 30 min at 4 $^{\circ}\text{C}$. Extracts were homogenized by sonication (Diagenode's Bioruptor, Diagenode, Liege, Belgium, 10 min, high power setting, 15 s on/30 s off), followed by centrifuging for 20 min at 13 000 r.p.m. The supernatant was transferred to a new tube and precleared by applying 40 μl of equilibrated Streptavidin-coupled Dynabeads (Invitrogen) for 20 min at 4 $^{\circ}\text{C}$. In order to block binding to unspecific RNA-binding proteins, 20 $\mu\text{g}/\text{ml}$ yeast RNA was

added and incubated for 20 min at 4 $^{\circ}\text{C}$. Biotinylated RNA (10 pmol) was heated for 5 min at 65 $^{\circ}\text{C}$, cooled down to room temperature and next incubated with 400 μg of precleared cellular extracts and 25 μl of equilibrated streptavidin-coupled Dynabeads (Invitrogen) for 2 h at 4 $^{\circ}\text{C}$. After washing four times for 5 min with RIP buffer, proteins were denatured in SDS buffer at 95 $^{\circ}\text{C}$ for 5 min and subjected to SDS-PAGE gels. Proteins were visualized by immunoblotting or by staining with SYPRO Ruby. Candidate protein bands were carefully cut out and sent out for mass spectrometric analysis. Specific mutations were produced using the QuikChange Multi Site-Directed Mutagenesis Kit (Agilent Technologies) as recommended by the manufacturer.

ChIP assays. ChIP assays were performed using anti-H3K4me3 (ab8580) from Abcam. Chromatin was sonicated to an average fragment size of 400–500 bp using the Diagenode Bioruptor. Rabbit IgG (Sigma, St. Louis, MO, USA) was used as a control for non-specific interactions. Input was prepared with 10% of the chromatin material used for immunoprecipitation. Input material was diluted 1:10 before PCR amplification. Quantification of immunoprecipitated DNA was performed by real-time PCR with the Applied Biosystems 7500 real-time PCR system (Applied Biosystems, Foster City, CA), using iTaq Universal SYBR Green Supermix (Bio-Rad). Sample quantifications by qPCR were performed in triplicate. Sequences of all oligonucleotides are provided in Supplementary Table S4.

RNA immunoprecipitation. Cellular extracts were prepared from NMuMG cells crosslinked with 1% formaldehyde. Cells were resuspended in RIP buffer and incubated 30 min at 4 $^{\circ}\text{C}$ and next were homogenized by sonication (Diagenode's Bioruptor, 10 min, high power setting, 15 s on/30 s off), and centrifuged for 20 min at 13 000 r.p.m. The supernatant was precleared by applying equilibrated protein A Dynabeads (Invitrogen) and non-specific competitor tRNA. Finally, 400 μg of extracts were incubated with 4 μg of antibody against U2AF65 (Abcam) and 100 μl of protein A Dynabeads for 3 h at 4 $^{\circ}\text{C}$. Beads were washed four times for 5 min at 4 $^{\circ}\text{C}$ with RIP buffer and resuspended in 100 μl of 50 mM Tris-Cl, pH 7.0, 5 mM EDTA, 10 mM DTT and 1% SDS and next were incubated at 70 $^{\circ}\text{C}$ for 45 min to reverse the crosslinks. RNA was extracted using TRIzol according to the manufacturer's protocol and was reverse transcribed and subjected to PCR analysis.

Cell fractionation. The separation of nuclear and cytosolic fractions was carried out using the PARIS Kit (Life Technologies) according to the manufacturer's instructions. RNA was extracted from each fraction using TRIzol reagent (Invitrogen).

Statistical analysis. Data were analyzed by one-way ANOVA and Student's *t*-test comparison, using GraphPad Prism 5 (Graphpad Software, La Jolla, CA, USA). Statistical significance was reached at $P < 0.05$.

Conflict of Interest

The authors declare no conflict of interest.

Acknowledgements. We thank Sharon von Weelden for technical help and Dr. A García de Herreros, Dr. A López-Rivas and Dr. M Encinas for providing valuable reagents. We are grateful to Dr. MA Moreno-Mateos, Dr. C Méndez-Vidal and Dr. JC Reyes for critical reading of the manuscript. This work was supported by grants from Ministerio de Economía y Competitividad (SAF2014-57632-P to JAP-T). CR-M was a recipient of a predoctoral fellowship from Ministerio de Economía y Competitividad.

1. Kalluri R, Weinberg RA. The basics of epithelial-mesenchymal transition. *J Clin Invest* 2009; **119**: 1420–1428.
2. Scheel C, Weinberg RA. Phenotypic plasticity and epithelial-mesenchymal transitions in cancer and normal stem cells? *Int J Cancer* 2011; **129**: 2310–2314.
3. Xu J, Lamouille S, Derynck R. TGF-beta-induced epithelial to mesenchymal transition. *Cell Res* 2009; **19**: 156–172.
4. Nieto MA. The ins and outs of the epithelial to mesenchymal transition in health and disease. *Annu Rev Cell Dev Biol* 2011; **27**: 347–376.
5. Thiery JP, Aclouque H, Huang RY, Nieto MA. Epithelial-mesenchymal transitions in development and disease. *Cell* 2009; **139**: 871–890.
6. Tam WL, Weinberg RA. The epigenetics of epithelial-mesenchymal plasticity in cancer. *Nat Med* 2013; **19**: 1438–1449.

7. Zheng H, Kang Y. Multilayer control of the EMT master regulators. *Oncogene* 2014; **33**: 1755–1763.
8. Shapiro IM, Cheng AW, Flytzanis NC, Balsamo M, Condeelis JS, Oktay MH et al. An EMT-driven alternative splicing program occurs in human breast cancer and modulates cellular phenotype. *PLoS Genet* 2011; **7**: e1002218.
9. Biamonti G, Bonomi S, Gallo S, Ghigna C. Making alternative splicing decisions during epithelial-to-mesenchymal transition (EMT). *Cell Mol Life Sci* 2012; **69**: 2515–2526.
10. Braeutigam C, Rago L, Rolke A, Waldmeier L, Christofori G, Winter J. The RNA-binding protein Rbfox2: an essential regulator of EMT-driven alternative splicing and a mediator of cellular invasion. *Oncogene* 2014; **33**: 1082–1092.
11. Warzecha CC, Jiang P, Amirikian K, Dittmar KA, Lu H, Shen S et al. An ESRP-regulated splicing programme is abrogated during the epithelial-mesenchymal transition. *EMBO J* 2010; **29**: 3286–3300.
12. Warzecha CC, Carstens RP. Complex changes in alternative pre-mRNA splicing play a central role in the epithelial-to-mesenchymal transition (EMT). *Semin Cancer Biol* 2012; **22**: 417–427.
13. Morris KV, Mattick JS. The rise of regulatory RNA. *Nat Rev Genet* 2014; **15**: 423–437.
14. Batista PJ, Chang HY. Long noncoding RNAs: cellular address codes in development and disease. *Cell* 2013; **152**: 1298–1307.
15. Mercer TR, Dinger ME, Mattick JS. Long non-coding RNAs: insights into functions. *Nat Rev Genet* 2009; **10**: 155–159.
16. Rinn JL, Chang HY. Genome regulation by long noncoding RNAs. *Annu Rev Biochem* 2012; **81**: 145–166.
17. Hu P, Yang J, Hou Y, Zhang H, Zeng Z, Zhao L et al. LncRNA expression signatures of twist-induced epithelial-to-mesenchymal transition in MCF10A cells. *Cell Signal* 2014; **26**: 83–93.
18. Ying L, Chen Q, Wang Y, Zhou Z, Huang Y, Qiu F. Upregulated MALAT-1 contributes to bladder cancer cell migration by inducing epithelial-to-mesenchymal transition. *Mol Biosyst* 2012; **8**: 2289–2294.
19. Luo M, Li Z, Wang W, Zeng Y, Liu Z, Qiu J. Long non-coding RNA H19 increases bladder cancer metastasis by associating with EZH2 and inhibiting E-cadherin expression. *Cancer Lett* 2013; **333**: 213–221.
20. Guo F, Parker Kerrigan BC, Yang D, Hu L, Shmulevich I, Sood AK et al. Post-transcriptional regulatory network of epithelial-to-mesenchymal and mesenchymal-to-epithelial transitions. *J. Hematol Oncol* 2014; **7**: 19.
21. Yuan JH, Yang F, Wang F, Ma JZ, Guo YJ, Tao QF et al. A Long noncoding RNA activated by TGF-beta promotes the invasion-metastasis cascade in hepatocellular carcinoma. *Cancer Cell* 2014; **25**: 666–681.
22. Huang S, Holzel M, Knijnenburg T, Schlicker A, Roepman P, McDermott U et al. MED12 controls the response to multiple cancer drugs through regulation of TGF-beta receptor signaling. *Cell* 2012; **151**: 937–950.
23. Kong L, Zhang Y, Ye ZQ, Liu XQ, Zhao SQ, Wei L et al. CPC: assess the protein-coding potential of transcripts using sequence features and support vector machine. *Nucleic Acids Res* 2007; **35**: W345–W349.
24. Wang L, Park HJ, Dasari S, Wang S, Kocher JP, Li W, CPAT. Coding-Potential Assessment Tool using an alignment-free logistic regression model. *Nucleic Acids Res* 2013; **41**: e74.
25. Deckers M, van Dinther M, Buijs J, Que I, Lowik C, van der Pluijm G et al. The tumor suppressor Smad4 is required for transforming growth factor beta-induced epithelial to mesenchymal transition and bone metastasis of breast cancer cells. *Cancer Res* 2006; **66**: 2202–2209.
26. Yu L, Hebert MC, Zhang YE. TGF-beta receptor-activated p38 MAP kinase mediates Smad-independent TGF-beta responses. *EMBO J* 2002; **21**: 3749–3759.
27. Shirakihara T, Saitoh M, Miyazono K. Differential regulation of epithelial and mesenchymal markers by deltaEF1 proteins in epithelial mesenchymal transition induced by TGF-beta. *Mol Biol Cell* 2007; **18**: 3533–3544.
28. Haynes J, Srivastava J, Madson N, Wittmann T, Barber DL. Dynamic actin remodeling during epithelial-mesenchymal transition depends on increased moesin expression. *Mol Biol Cell* 2011; **22**: 4750–4764.
29. Inman GJ, Nicolas FJ, Callahan JF, Harling JD, Gaster LM, Reith AD et al. SB-431542 is a potent and specific inhibitor of transforming growth factor-beta superfamily type I activin receptor-like kinase (ALK) receptors ALK4, ALK5, and ALK7. *Mol Pharmacol* 2002; **62**: 65–74.
30. Orom UA, Shiekhattar R. Long non-coding RNAs and enhancers. *Curr Opin Genet Dev* 2011; **21**: 194–198.
31. Goff LA, Rinn JL. Linking RNA biology to lncRNAs. *Genome Res* 2015; **25**: 1456–1465.
32. Thuault S, Tan EJ, Peinado H, Cano A, Heldin CH, Moustakas A. HMGA2 and Smads co-regulate SNAIL1 expression during induction of epithelial-to-mesenchymal transition. *J Biol Chem* 2008; **283**: 33437–33446.
33. Thuault S, Valcourt U, Petersen M, Manfioletti G, Heldin CH, Moustakas A. Transforming growth factor-beta employs HMGA2 to elicit epithelial-mesenchymal transition. *J Cell Biol* 2006; **174**: 175–183.
34. Shirakihara T, Horiguchi K, Miyazawa K, Ehata S, Shibata T, Morita I et al. TGF-beta regulates isoform switching of FGFR receptors and epithelial-mesenchymal transition. *EMBO J* 2011; **30**: 783–795.
35. Horiguchi K, Sakamoto K, Koinuma D, Semba K, Inoue A, Inoue S et al. TGF-beta drives epithelial-mesenchymal transition through deltaEF1-mediated downregulation of ESRP. *Oncogene* 2012; **31**: 3190–3201.
36. Lamouille S, Xu J, Derynck R. Molecular mechanisms of epithelial-mesenchymal transition. *Nat Rev* 2014; **15**: 178–196.
37. Gonzalez DM, Medici D. Signaling mechanisms of the epithelial-mesenchymal transition. *Sci Signal* 2014; **7**: re8.
38. Ramos AD, Andersen RE, Liu SJ, Nowakowski TJ, Hong SJ, Gertz CC et al. The long noncoding RNA Pnky regulates neuronal differentiation of embryonic and postnatal neural stem cells. *Cell Stem Cell* 2015; **16**: 439–447.
39. Guttman M, Donaghey J, Carey BW, Garber M, Grenier JK, Munson G et al. lincRNAs act in the circuitry controlling pluripotency and differentiation. *Nature* 2011; **477**: 295–300.
40. Liang WC, Fu WM, Wong CW, Wang Y, Wang WM, Hu GX et al. The LncRNA H19 promotes epithelial to mesenchymal transition by functioning as miRNA sponges in colorectal cancer. *Oncotarget* 2015; **6**: 22513–22525.
41. Richards EJ, Zhang G, Li ZP, Permeth-Wey J, Challa S, Li Y et al. Long non-coding RNAs (lncRNA) regulated by transforming growth factor (TGF) beta: lncRNA-hit-mediated TGFbeta-induced epithelial to mesenchymal transition in mammary epithelia. *J Biol Chem* 2015; **290**: 6857–6867.
42. Derynck R, Smad-dependent Zhang YE. and Smad-independent pathways in TGF-beta family signalling. *Nature* 2003; **425**: 577–584.
43. Orom UA, Derrien T, Beringer M, Gumireddy K, Gardini A, Bussotti G et al. Long noncoding RNAs with enhancer-like function in human cells. *Cell* 2010; **143**: 46–58.
44. Engreitz JM, Haines JE, Perez EM, Munson G, Chen J, Kane M et al. Local regulation of gene expression by lncRNA promoters, transcription and splicing. *Nature* 2016; **539**: 452–455.
45. Mazzon M, Jones M, Davidson A, Chain B, Jacobs M. Dengue virus NS5 inhibits interferon-alpha signaling by blocking signal transducer and activator of transcription 2 phosphorylation. *J Infect Dis* 2009; **200**: 1261–1270.
46. Impagnatiello MA, Weitzer S, Gannon G, Compagni A, Cotten M, Christofori G. Mammalian sprouty-1 and -2 are membrane-anchored phosphoprotein inhibitors of growth factor signaling in endothelial cells. *J Cell Biol* 2001; **152**: 1087–1098.
47. Bronnum H, Andersen DC, Schneider M, Sandberg MB, Eskildsen T, Nielsen SB et al. miR-21 promotes fibrogenic epithelial-to-mesenchymal transition of epicardial mesothelial cells involving Programmed Cell Death 4 and Sprouty-1. *PLoS ONE* 2013; **8**: e56280.
48. Capaccione KM, Hong X, Morgan KM, Liu W, Bishop JM, Liu L et al. Sox9 mediates Notch1-induced mesenchymal features in lung adenocarcinoma. *Oncotarget* 2014; **5**: 3636–3650.
49. Kondo M, Cubillo E, Tobiume K, Shirakihara T, Fukuda N, Suzuki H et al. A role for Id in the regulation of TGF-beta-induced epithelial-mesenchymal transdifferentiation. *Cell Death Differ* 2004; **11**: 1092–1101.
50. Battle E, Sancho E, Franci C, Dominguez D, Morfar M, Baulida J et al. The transcription factor snail is a repressor of E-cadherin gene expression in epithelial tumour cells. *Nat Cell Biol* 2000; **2**: 84–89.
51. Tripathi V, Ellis JD, Shen Z, Song DY, Pan Q, Watt AT et al. The nuclear-retained non-coding RNA MALAT1 regulates alternative splicing by modulating SR splicing factor phosphorylation. *Mol Cell* 2010; **39**: 925–938.
52. Gonzalez I, Munita R, Agirre E, Dittmer TA, Gysling K, Misteli T et al. A lncRNA regulates alternative splicing via establishment of a splicing-specific chromatin signature. *Nat Struct Mol Biol* 2015; **22**: 370–376.
53. Bebee TW, Park JW, Sheridan KI, Warzecha CC, Cieply BW, Rohacek AM et al. The splicing regulators Esrp1 and Esrp2 direct an epithelial splicing program essential for mammalian development. *Elife* 2015; **4**: e088954.

Supplementary Information accompanies this paper on Cell Death and Differentiation website (<http://www.nature.com/cdd>)